Control of sympathetic vasomotor tone by catecholaminergic C1 neurones of the rostral ventrolateral medulla oblongata

Nephtali Marina[1], Ana P.L. Abdala[2], Alla Korsak[1], Annabel E. Simms[3]†, Andrew M. Allen[3], Julian F.R. Paton[2], and Alexander V. Gourine[1]*

[1]Neuroscience, Physiology and Pharmacology, University College London, Gower Street, London WC1E 6BT, UK; [2]School of Physiology and Pharmacology, Bristol Heart Institute, Medical Sciences Building, University of Bristol, Bristol BS8 1TD, UK; and [3]Department of Physiology, Faculty of Medicine, Dentistry and Health Sciences, University of Melbourne, Melbourne, Victoria 3010, Australia

Aims	Increased sympathetic tone in obstructive sleep apnoea results from recurrent episodes of systemic hypoxia and hypercapnia and might be an important contributor to the development of cardiovascular disease. In this study, we re-evaluated the role of a specific population of sympathoexcitatory catecholaminergic C1 neurones of the rostral ventrolateral medulla oblongata in the control of sympathetic vasomotor tone, arterial blood pressure, and hypercapnia-evoked sympathetic and cardiovascular responses.
Methods and results	In anaesthetized rats *in vivo* and perfused rat working heart brainstem preparations *in situ*, C1 neurones were acutely silenced by application of the insect peptide allatostatin following cell-specific targeting with a lentiviral vector to express the inhibitory *Drosophila* allatostatin receptor. In anaesthetized rats with denervated peripheral chemoreceptors, acute inhibition of 50% of the C1 neuronal population resulted in ∼50% reduction in renal sympathetic nerve activity and a profound fall in arterial blood pressure (by ∼25 mmHg). However, under these conditions systemic hypercapnia still evoked vigorous sympathetic activation and the slopes of the CO_2-evoked sympathoexcitatory and cardiovascular responses were not affected by inhibition of C1 neurones. Inhibition of C1 neurones *in situ* resulted in a reversible fall in perfusion pressure and the amplitude of respiratory-related bursts of thoracic sympathetic nerve activity.
Conclusion	These data confirm a fundamental physiological role of medullary catecholaminergic C1 neurones in maintaining resting sympathetic vasomotor tone and arterial blood pressure. However, C1 neurones do not appear to mediate sympathoexcitation evoked by central actions of CO_2.
Keywords	Sympathetic • Arterial blood pressure • Obstructive sleep apnoea • Hypercapnia • Lentivirus

1. Introduction

Obstructive sleep apnoea is a major public health problem affecting ∼5% of the world's population.[1] Obstructive sleep apnoea often has no clear manifestations and remains undiagnosed until daytime somnolence and cognitive problems become evident. Repetitive and prolonged obstructions of the airways during sleep result in recurrent periods of hypoxia (decrease in arterial PO_2), hypercapnia (increase in arterial PCO_2) and arousal leading to increased sympathetic tone, endothelial damage and dysfunction.[2,3] These changes may lead to cardiovascular pathology, including hypertension,[4,5] coronary artery disease,[6] and cerebrovascular disease.[7,8] Understanding the

mechanisms of sympathetic activation in sleep apnoea requires detailed knowledge of the central and peripheral mechanisms underlying sympathetic control at rest and during hypoxia and hypercapnia.

Sympathetic vasomotor and cardiac neural activities are produced by the sympathetic preganglionic neurones in the spinal cord which receive tonic excitatory drive from supraspinal regions within the brainstem and the hypothalamus.[9–14] These regions include the rostral ventrolateral medulla (RVLM), rostral ventromedial and midline medulla, the A5 cell group of the pons and the paraventricular hypothalamic nucleus.[9,15] The RVLM is believed to contribute significantly to the generation of sympathetic vasomotor tone[9–11,13,14] since in anaesthetized experimental animals acute bilateral inactivation or ablation of the RVLM neurones leads to a fall in arterial pressure and sympathetic activity to the levels observed after transection of the spinal cord or during ganglionic blockade.[9,16,17] Sympathoexcitatory RVLM neurones are composed of two groups: a subgroup of the C1 catecholaminergic neurones (they contain enzymes necessary to produce adrenaline) and non-catecholaminergic, presumably glutamatergic neurons.[10,11,13,17–19]

Increases in the level of arterial PCO_2 are known to evoke robust increases in sympathetic activity,[20] but the mechanisms by which this occurs are not entirely clear. RVLM neurones, including C1 cells, are spontaneously active and show increased activity during hypercapnia *in vivo*.[21] C1 neurones, however, do not appear to be intrinsically chemosensitive showing no responses to changes in pH (which follow changes in PCO_2) when studied *in vitro*.[22,23] Previous studies have demonstrated that permanent depletion of catecholaminergic C1 neurones (>75%) abolishes sympathoexcitation induced by activation of peripheral chemoreceptors.[24] However, the contribution of C1 neurones to the increases in sympathetic activity evoked by central actions of CO_2 has not been characterized.

In this study, we targeted C1 neurones with a lentiviral construct to express *Drosophila* allatostatin receptor (AlstR).[25] Activation of AlstR by allatostatin peptide opens G-protein-coupled inward-rectifying potassium channels, resulting in a strong and reversible neuronal hyperpolarization.[26–28] Naturally, allatostatin receptors are only expressed in insects and allatostatin itself does not have apparent biological activity in mammals.[25,27] Given a significant cellular expression of AlstR is achieved, application of allatostatin can be used for immediate and reversible inhibition of targeted CNS neurones.

Here, we used this approach to acutely inhibit C1 neurones both *in vivo* (in anaesthetized and artificially ventilated adult rats with denervated peripheral chemoreceptors) and *in situ* (in arterially perfused brainstem preparations) to determine the contribution of this neuronal population to the generation of resting sympathetic activity. The role of the C1 group in the development of sympathoexcitatory responses to systemic hypercapnia was also determined in the *in vivo* experiments.

2. Methods

All the experiments were performed in accordance with the European Commission Directive 86/609/EEC (European Convention for the Protection of Vertebrate Animals used for Experimental and Other Scientific Purposes), the UK Home Office (Scientific Procedures) Act (1986), or the National Health and Medical Research Council of Australia 'Guidelines to promote the wellbeing of animals used for scientific purposes' with project approval from the University College London, University of Bristol and University of Melbourne Institutional Animal Ethics Committees.

2.1 Viral vectors

Catecholaminergic brainstem neurones characteristically express transcriptional factor Phox2 and, therefore, can be targeted using viral vectors to express the gene of interest under the control of an artificial promoter PRSx8—Phox2-activated promoter.[29–31] The lentiviral vector (LVV) system used here was HIV-1-derived and pseudo-typed with the VSV-G envelope.[32] The plasmid pTYF-PRSx8-AlstR-IRES2-EGFP was cloned into the LVV. Titres of PRSx8-AlstR-EGFP-LV and the control virus (PRSx8-EGFP-LV) were between 1×10^9 and 1×10^{10} pfu. Viral concentration and titration were performed as described in detail previously.[32]

2.2 *In vivo* gene transfer

Post-weaned male Sprague Dawley or Wistar rats (50–80 g) were anaesthetized with a mixture of ketamine (60 mg kg^{-1}; i.m.) and medetomidine (250 µg kg^{-1}, i.m.). Animals were placed in a stereotaxic frame and two microinjections per side of PRSx8-AlstR-EGFP-LV or PRSx8-EGFP-LV (0.25 µL each) were delivered into the rostral ventrolateral reticular formation of the medulla oblongata. The microinjection pipette was angled and positioned $\pm$ 1.7 mm lateral from the midline. The exact RVLM coordinates (adapted to our stereotaxic apparatus) in these young rats were determined in dedicated preliminary trials using microinjections of fluorescent beads with subsequent histological analysis to verify the sites of delivery. Anaesthesia was reversed with atipemazole (1 mg kg^{-1}).

2.3 *In vivo* experiments

Five to six weeks after the injections, Sprague Dawley rats were anaesthetized with urethane (1.15 g kg^{-1} i.v., supplemented with 5–10 mg i.v. as required) following femoral vein cannulation under isoflurane (3%) induction (experiments conducted at the University College London). The depth of anaesthesia was monitored using the stability of blood pressure, heart rate, and lack of flexor responses to a paw-pinch. The femoral artery was cannulated for recordings of the arterial blood pressure. Body temperature was kept constant at $37.0 \pm 0.2°C$. The trachea was cannulated and the animal was ventilated artificially (frequency 1 Hz, volume 2–2.5 mL) with O_2-enriched air (~30% O_2). The end-tidal level of CO_2 was monitored continuously (Capstar-100, CWE, Inc., USA); arterial PCO_2, PO_2, and pH were measured regularly. The left renal nerve was dissected retroperitoneally and its activity was recorded using implanted bipolar silver electrodes. Carotid sinus and aortic nerves were sectioned to eliminate inputs from the peripheral chemoreceptors and arterial baroreceptors. Effective peripheral chemodenervation was confirmed at the end of each experiment by monitoring lack of the respiratory response to a brief bout of systemic hypoxia (lowering O_2 in the inspired gas mixture to 10%).

It has been shown previously that allatostatin is capable of diffusing deep into the brain tissue reaching neurones of the respiratory rhythm-generating circuits even after administration into the IV cerebral ventricle.[33] To aid delivery of allatostatin to the transduced C1 neurones located in the rostroventrolateral aspect of the medullary reticular formation, the ventral surface of the medulla oblongata (VMS) was exposed as described previously.[34] Artificial cerebrospinal fluid (aCSF; saturated with 95% O_2/5% CO_2, pH 7.4) or allatostatin (10 µM in aCSF; Ser-Arg-Pro-Tyr-Ser-Phe-Gly-Leu-NH$_2$, Phoenix Pharmaceuticals, USA) was applied to the VMS of rats transduced with PRSx8-AlstR-EGFP-LV ($n = 8$) or PRSx8-EGFP-LV ($n = 3$). All the animals were subjected to the same experimental interventions in the following sequence: the renal sympathetic nerve activity (SNA), blood pressure, and heart rate responses to increased level of CO_2 in inspired air were first determined 5 min after application of aCSF, followed by two subsequent CO_2 challenges, one after at least 30 min recovery

period and 5 min after application of allatostatin on the VMS (the effect of allatostatin on SNA and cardiovascular variables was assessed at the same time), and another after allatostatin washout from the VMS by 60 min of continuous aCSF superfusion ($n = 8$). Following recovery (at least 60 min), animals were subjected to another CO_2 challenge and the effect of allatostatin on the PRSx8-AlstR-EGFP-LV transduced brainstem was also tested at the peak of the CO_2-evoked sympathoexcitatory response ($n = 8$).

A separate experiment was conducted to determine whether the effects of allatostatin were mediated in part via inhibition of the neighbouring glutamatergic chemosensitive neurones of the retrotrapezoid nucleus (RTN). Some of the chemosensitive RTN neurones express Phox2b and may have been transduced also due to spill over of the PRSx8-AlstR-EGFP-LV from the site of injection. Glutamatergic excitatory inputs to the RVLM, including these from the RTN were blocked by application of ionotropic excitatory amino acid receptor antagonist kynurenic acid (Kyn, 50 mM) on the VMS. Next, CO_2 was added to the inspired gas mixture, and allatostatin was applied at the peak of the hypercapnic response as described above.

2.4 *In situ* experiments

Experiments using *in situ* perfused working heart brainstem-spinal cord preparations[35–37] were conducted to complement the data obtained using *in vivo* preparations. The main objective was to determine the effect of allatostatin-evoked inhibition of C1 neurones on SNA in the absence of anaesthetics. Briefly, 8–10 days after the injections of the viral vectors, Wistar rats (experiments conducted at the University of Melbourne) were deeply anaesthetized with isoflurane until loss of paw withdrawal reflex, bisected below the diaphragm, exsanguinated, immersed in cold carbogenated Ringer solution, and decerebrated precollicularly. Lungs were removed and the descending aorta was isolated and cleaned. Preparations were transferred to a recording chamber and a double lumen cannula was placed into the descending aorta for retrograde perfusion with a Ringer solution containing in mM: NaCl (125), NaHCO$_3$ (24), KCl (3), CaCl$_2$ (2.5), MgSO$_4$ (1.25), KH$_2$PO$_4$ (1.25), and D-glucose (10). Ficoll (MWt 20 000; 1.25%) was added as an oncotic agent and the perfusion solution was saturated with 95% O$_2$-5% CO$_2$ (pH 7.35–7.4; osmolality 290 ± 5 mosm kg H$_2$O^{-1} at 31°C). Carotid and aortic bodies inputs were left intact. Neuromuscular blockade was achieved using vecuronium bromide added to the perfusate ($2-4$ μg mL^{-1}). Phrenic nerve (PNA) and thoracic sympathetic nerve (tSNA) activities were simultaneously recorded. Signals were amplified ($\times 20$k), filtered (50–1500 Hz), digitized, and recorded using *Spike 2* software (CED, Cambridge, UK).

Allatostatin (1 μM) was added to the perfusate for 10–15 min. Fresh perfusate was used to washout the peptide. Since *in vivo* experiments (see *Results* below) demonstrated that C1 neurones are unlikely to be responsible for the increases in sympathetic drive evoked by central actions of CO_2, hypercapnia-evoked responses were not re-tested.

2.5 Immunohistochemistry

At the end of the *in vivo* experiments, animals were perfused transcardially with 0.9% NaCl solution followed by 500 mL of 4% paraformaldehyde (PFA). Brainstems were removed, post-fixed for 12 h in 4% PFA at 4°C and cryoprotected in 30% sucrose. Medulla oblongata was sectioned using a freezing microtome, and a series of coronal sections (30 μm) was collected and stored in anti-freeze at $-20°C$ for subsequent histological processing. Sections were immunostained for detection of tyrosine hydroxylase (TH; marker of catecholaminergic neurones) and EGFP. Immunohistochemical detection of the latter was necessary for positive identification of the transduced neurones, because in our preliminary trials we found weak EGFP fluorescence following transduction with PRSx8-AlstR-EGFP-LV. Tissue was incubated in chicken anti-GFP antibody (1:250, Avés) for 48 h followed by sheep anti-TH antiserum for 24 h

(1:250, Abcam). Secondary antibodies were goat anti-chicken Alexa 568 (1:1000, Molecular probes) and biotinilated goat anti-sheep (1:500) amplified by fluorescein avidin DCS (1:250, Vector laboratories).

2.6 Autoradiography

The distribution of transgenic allatostatin receptor expression was examined using an autoradiography protocol modified from.[38] The brains were removed, snap-frozen in iso-pentane cooled on dry ice, and 20 μm coronal sections were cut using a cryostat at $-20°C$, mounted on gelatine-coated slides and desiccated at 4°C prior to storage at $-80°C$. Sections were incubated for 20 min in a buffer containing 10 mM HEPES, 5 mM MgCl$_2$, 1 mM phenylmethanesulfonyl fluoride, 1 mM EGTA, 1 mM O-phenanthroline (pH 7.4) at room temperature followed by incubation for 1 h in the same buffer containing 10 mg mL^{-1} BSA and ^{125}I-allatostatin (90 pM; iodinated by ProSearch International, Australia). To determine the level of non-specific binding, some sections were incubated with 1 μM of unlabelled allatostatin. Sections were washed, air dried and exposed to X-ray film for 3–4 weeks. ^{125}I-radioactivity standards were also included to enable calibration of binding density. Following exposure, sections on the autoradiographs were scanned and images were analysed to determine optical densities of the binding areas using Scion Image Software (Scion Corp, USA).

## 2.7 Data acquisition and analysis

Renal SNA, blood pressure, and tracheal pressure were recorded using a Power 1401 interface and *Spike2* software. SNA was amplified ($\times 20$ 000), filtered (80–800 Hz), and sampled at a rate of 11 kHz. Physiological data were digitized and analysed offline (*Spike2*). Heart rate was derived from the blood pressure traces. Rectified SNA sampled at 100 Hz was smoothed with a time constant of 10 s to obtain mean level (ML) of activity. CO_2 and allatostatin-evoked changes in RSNA were normalized with respect to resting activity in normoxia/normocapnia (100%) and complete the absence of discharges (0%) following administration of the ganglionic blocker hexamethonium (20 mg; i.v.). The data are expressed as means $\pm$ SE and were compared using Student's paired *t*-test. A *P*-value of less than 0.05 was considered to be significant.

In the *in situ* experiments, tSNA was analysed offline (*Spike2*) using customized scripts. Rectified tSNA was smoothed with a time constant of 50 ms and MLs were taken from a 2 min time period. Phrenic triggered averaging across 20 respiratory cycles was carried out to determine the amplitude of the respiratory-related bursts of tSNA before and after allatostatin application.

Distribution of EGFP-immunoreactive (EGFP-IR) and TH-IR neurones was analysed using epifluorescence microscopy. Colocalization of EGFP with TH was determined by visual inspection through a $\times 20$ objective. Cell counting was performed manually using a one in three series of 30 μm sections of the brainstem. TH positive cells transduced with AlstR-EGFP were counted on both sides of the brain regardless of staining intensity, and cell numbers were summed. Efficacy of the transduction is expressed as a percentage of TH-IR neurones expressing AlstR-EGFP located in the rostral ventrolateral reticular formation of the medulla oblongata $\sim 11.3-12.8$ mm caudal to Bregma (*Figure 1A*). Anatomical reconstruction of transduced neurones in a representative brainstem was performed manually using Paxinos and Watson stereotaxic atlas as a guide (*Figure 1B*).

3. Results

Transduction efficacy was examined in the brainstems of all the animals by immunohistochemical detection of EGFP and TH co-localization or by autoradiographic detection of allatostatin receptor binding (*Figure 1*). EGFP immunostaining revealed bilateral clusters of AlstR-EGFP-expressing neurones in the rostral ventrolateral reticular formation of the medulla oblongata (between 11.3 and 12.8 mm
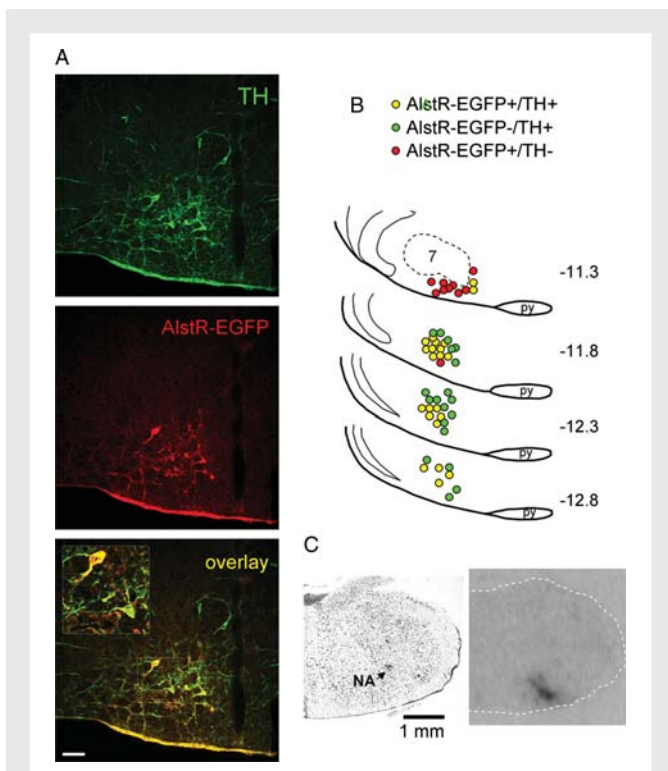
Figure 1 Targeting catecholaminergic C1 neurones in the rostral ventrolateral medulla oblongata (RVLM) with PRSx8-AlstR-EGFP-LV (A) Confocal images of tyrosine hydroxylase (TH)-positive neurones (green) expressing AlstR-EGFP (red). Bregma level -12.8 mm. Scale bar = 50 μm. (B) Distribution of TH-immunoreactive neurones expressing AlstR-EGFP in one representative rat brainstem 5 weeks after microinjection of PRSx8-AlstR-EGFP-LV into the RVLM. Each symbol represents three neurones. Numbers indicate distances from Bregma. 7, facial motor nucleus; py, pyramidal tract. (C) Binding of ^{125}I-allatostatin in the rat RVLM 9 days after microinjection of PRSx8-AlstR-EGFP-LV. Left, Nissl stain; right, autoradiography image showing strong AlstR binding in the rostral ventrolateral reticular formation. NA, nucleus ambiguus.

caudal to Bregma, *Figure 1B*). EGFP-IR was present both in the soma and dendritic processes of the transduced TH-positive neurones (*Figure 1A*). The distribution of transduced neurones in a representative brainstem is illustrated in *Figure 1B*. AlstR-EGFP expression was found in $51 \pm 7\%$ ($n = 12$) of all identified TH-positive RVLM neurones, confirming effective targeting of the C1 neuronal population with PRSx8-AlstR-EGFP-LV. A scatter of EGFP-expressing neurones showing no immunoreactivity for TH was also found in the ventrolateral reticular formation immediately rostral to the caudal border of the facial nucleus corresponding to the anatomical location of the RTN (*Figure 1B*).

Strong ^{125}I-allatostatin binding was detected bilaterally in all the animals injected with PRSx8-AlstR-EGFP-LV within the same rostrocaudal distribution as described above (*Figure 1C*). No specific AlstR binding was observed in the RVLM of naïve rats, animals injected with PRSx8-EGFP-LV, or after incubation of the slices with excess amount (1 μM) of unlabelled allatostatin (data not shown) indicating high affinity and specific binding.

In anaesthetized, peripheral chemo- and baro-denervated and artificially ventilated rats transduced with PRSx8-AlstR-EGFP-LV into the

RVLM ($n = 8$), application of allatostatin (10 μM) onto the VMS in normoxia/normocapnia resulted in immediate and profound reductions in resting RSNA (by $51 \pm 5\%$; $P = 0.009$; *Figure 2*), mean ABP (MABP; by 25.4 ± 3.9 mmHg; $P = 0.0003$; *Figure 2A* and *C*), and heart rate (by 41 ± 7 b.p.m.; $P = 0.0003$). Allatostatin (0.01–2 mM) had no effect on RSNA, MABP, or heart rate in animals transduced with PRSx8-EGFP-LV ($n = 3$; *Figure 2C*) or injected with PRSx8-AlstR-EGFP-LV rostral to the RVLM (~9.5 mm from Bregma) and showing no transgene expression in the C1 region ($n = 5$; data not shown). Therefore, allatostatin does not appear to cross-react with endogenous targets within the rat brainstem presympathetic circuits.

Rising levels of inspired CO_2 in rats with denervated peripheral chemoreceptors ($n = 8$) induced an increase in RSNA (by $80 \pm 20\%$; $P = 0.002$) and MABP (by 23.7 ± 6.6 mmHg; $P = 0.004$) (*Figure 3*). The heart rate was not significantly affected during hypercapnia ($P = 0.206$). Similar CO_2-evoked increases in RSNA (by $74.6 \pm 15\%$; $P = 0.0006$) and MABP (by 22.1 ± 6.8 mm Hg; $P = 0.008$) were observed in the presence of allatostatin on the VMS of transduced rats (*Figure 3*). However, these responses were mounted from the lower levels of RSNA and arterial blood pressure achieved by allatostatin-evoked inhibition of the RVLM circuits (*Figure 3B*). Although peak CO_2-evoked increases in RSNA and MABP were significantly smaller in comparison with those evoked during hypercapnia in control conditions ($P = 0.004$ and $P = 0.006$, respectively), the slopes of the responses to CO_2 were similar before and after application of allatostatin on the VMS of rats transduced with PRSx8-AlstR-EGFP-LV (*Figure 3B*).

Inhibition of the transduced RVLM neurones by allatostatin applied on the VMS at the peak of the CO_2-evoked sympathoexcitatory response resulted in a significant reduction in RSNA (by $72.0 \pm 1.5\%$; $n = 8$; $P = 0.003$), MABP (by 36.3 ± 4.8 mm Hg; $n = 8$; $P = 0.0003$) and HR (by 26 ± 7 b.p.m.; $n = 8$; $P = 0.0008$) (*Figure 4*). In conditions of RVLM ionotropic excitatory amino acid receptor blockade following application of Kyn (50 mM) on the VMS, hypercapnia was still effective in triggering increases in RSNA and MABP (*Figure 4C*), while subsequent allatostatin application effectively reduced RSNA by $24 \pm 2\%$ ($n = 3$; $P = 0.015$) and MABP by 15 ± 5 mmHg ($n = 3$; $P = 0.025$) (*Figure 4C*).

In the perfused working heart brainstem preparations of rats transduced with PRSx8-AlstR-EGFP-LV into the RVLM ($n = 7$), addition of allatostatin (1 μM) to the perfusate caused a significant fall in the perfusion pressure (by 6.3 ± 1.2 mm Hg; $P = 0.003$), reduction in the amplitude of the Hering–Traube pressure waves and respiratory-related tSNA bursts (by 29%; $P = 0.047$, *Figure 5*). The timing of the post-inspiratory peaks in tSNA was not altered by inhibition of the RVLM circuits (*Figure 5B*). Allatostatin added to the perfusate of rats which had not been injected with a viral vector ($n = 3$) or had been injected with PRSx8-EGFP-LV ($n = 2$) had no effect on perfusion pressure, HR, or tSNA (data not shown). On wash out of allatostatin a full recovery in perfusion pressure, amplitude of the Hering–Traube waves and sympathetic discharge pattern was observed (*Figure 5A*).

4. Discussion

In the present study, we used a LVV to express inhibitory *Drosophila* allatostatin receptor in a population of the RVLM catecholaminergic C1 neurones in order to determine the role of these neurones in
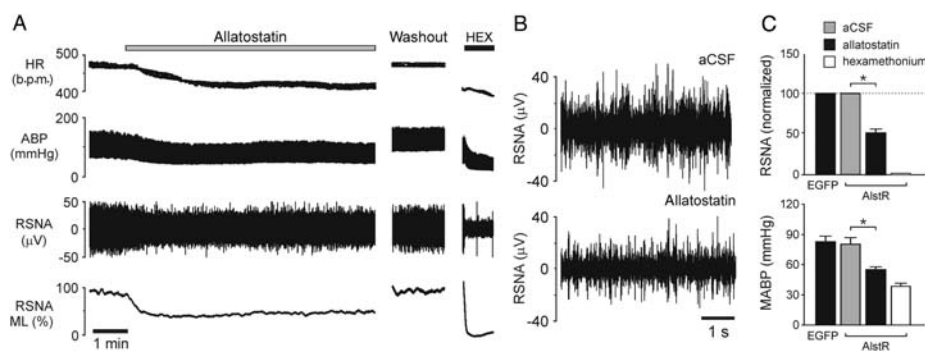
Figure 2 Effect of acute inhibition of AlstR-expressing ventrolateral brainstem neurones on sympathetic nerve activity, arterial blood pressure, and heart rate *in vivo*. (*A*) Representative recording illustrating changes in resting heart rate (HR), arterial blood pressure (ABP), renal sympathetic nerve activity (RSNA) and mean level (ML) of RSNA in response to allatostatin (10 μM) application on the ventral surface of the medulla oblongata (VMS) in an animal transduced with PRSx8-AlstR-EGFP-LV into the RVLM (anaesthetized and artificially ventilated rat with denervated carotid and aortic bodies). HEX, hexamethonium. (*B*) Expanded records of raw RSNA before and after application of allatostatin on the VMS in an animal from the example shown in (*A*). (*C*) Summary data showing changes in RSNA and mean ABP (MABP) 5 min after allatostatin application on the VMS in animals transduced with PRSx8-AlstR-EGFP-LV (AlstR) or PRSx8-EGFP-LV (EGFP) (*$P < 0.05$).
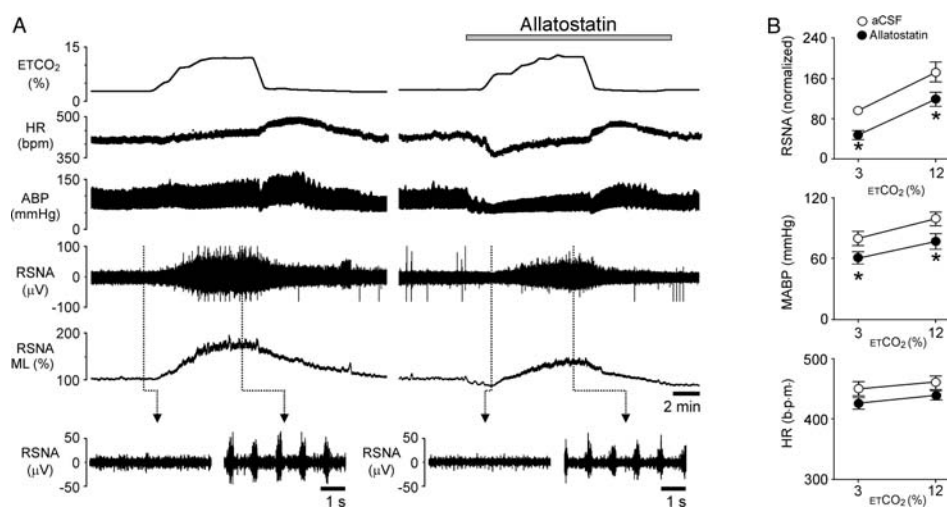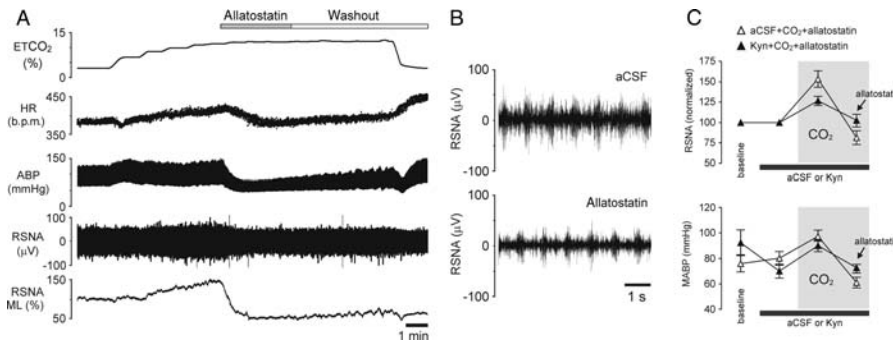

Figure 3 Effect of acute inhibition of AlstR-expressing ventrolateral brainstem neurones on CO_2-evoked sympathetic and cardiovascular responses *in vivo*. (*A*) Representative time-condensed recording illustrating changes in HR, ABP, RSNA, and ML of RSNA in response to repeated increases in the level of inspired CO_2 in the absence and presence of allatostatin (10 μM) on the VMS. Rat was transduced with PRSx8-AlstR-EGFP-LV into the RVLM, anaesthetized, peripherally chemodenervated and artificially ventilated. ETCO$_2$, end-tidal CO_2. (*B*) Summary data illustrating slopes of the CO_2-evoked increases in RSNA, MABP, and HR in the absence and presence of allatostatin on the VMS in rats transduced with PRSx8-AlstR-EGFP-LV into the RVLM. Asterisk indicates significant differences in RSNA or MABP before and after application of allatostatin in normo- and hypercapnia, $P < 0.05$.

the control of resting sympathetic activity, arterial blood pressure, heart rate, and CO_2-evoked sympathoexcitatory and cardiovascular responses. Acute inhibition of approximately half of the C1 neuronal population resulted in a $\sim$50% reduction in renal sympathetic activity and a substantial fall in the arterial blood pressure suggesting that these neurones are essential for the maintenance of resting sympathetic vasomotor tone. The data obtained also suggest that the RVLM C1 neurones are unlikely to be responsible for the increases in sympathetic drive evoked by central actions of CO_2.

The role of C1 neurones in the regulation of sympathetic activity and arterial blood pressure was addressed previously by Schreihofer

and Guyenet[24] who used anti-dopamine-beta-hydroxylase antibody conjugated to ribosomal toxin saporin to produce permanent lesions of the brainstem catecholaminergic neurones, including C1 cell group. This approach was effective in causing loss of >75% of C1 neurones but also lesions of the other bulbospinal catecholaminergic cell groups. However, resting SNA and blood pressure were unaffected.[24] These results are in odds with the data obtained in the present study and indicate that on a longer time-scale other populations of sympathoexcitatory neurones (e.g. non-catecholaminergic RVLM bulbospinal neurones, or sympathoexcitatory neurones of the hypothalamus and other regions of the brainstem) may effectively

Figure 4 Effect of acute inhibition of AlstR-expressing ventrolateral brainstem neurones on sympathetic nerve activity and arterial blood pressure in conditions of enhanced sympathetic drive during hypercapnia *in vivo*. (*A*) Representative recording illustrating changes in HR, ABP, RSNA and ML, or RSNA in response to allatostatin (10 μM) applied on the VMS at the peak of the CO_2-evoked sympathetic and cardiovascular responses in an animal transduced with PRSx8-AlstR-EGFP-LV (anaesthetized, peripherally chemodenervated and artificially ventilated rat). (*B*) Expanded records of raw RSNA during hypercapnia before and after application of allatostatin on the VMS in an animal from the example shown in (*A*). (*C*) Summary data showing changes in RSNA and MABP induced by allatostatin application on the VMS in conditions of ionotropic excitatory amino acid receptor blockade by kynurenic acid (Kyn, 50 mM) in hypercapnic animals transduced with PRSx8-AlstR-EGFP-LV. Grey boxes depict periods of hypercapnia.
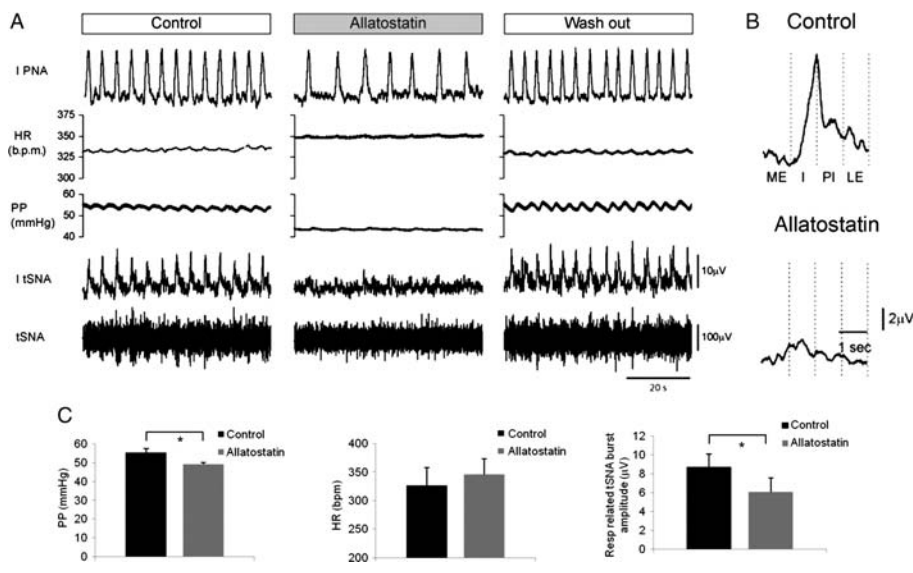
Figure 5 Effect of acute inhibition of AlstR-expressing ventrolateral brainstem neurones on sympathetic nerve activity and perfusion pressure in the *in situ* working heart brainstem preparation. (*A*) Representative raw data illustrating changes in thoracic sympathetic nerve activity (tSNA) and perfusion pressure (PP) in response to addition of allatostatin (1 μM) to perfusate in a rat preparation transduced into the RVLM with PRSx8-AlstR-EGFP-LV. IPNA, integrated phrenic nerve activity. (*B*) Phrenic-triggered averages of tSNA across 20 respiratory cycles before and after application of allatostatin. The amplitude, represented in *C* is taken as the peak to trough of these averages. Note that the timing of the peak of tSNA is not altered by allatostatin and occurs during post-inspiration (PI). ME, mid-expiration; I, inspiration; LE, late inspiration. (*C*) Summary data showing the effect of allatostatin on the PP, HR, and the amplitude of the respiratory-related tSNA bursts ($n = 7$; $*P < 0.05$).

compensate for the gradual but permanent loss of the C1 group. Recent studies involving direct and specific stimulation of the genetically targeted RVLM C1 neurones confirmed that their activation increases SNA and arterial blood pressure.[31,39]

Histological analysis revealed that in our experiments at least 51% of TH-positive RVLM neurones were transduced, suggesting that lentiviral targeting results in a significant AlstR-EGFP expression among catecholaminergic RVLM neurones. The expression of AlstR-binding sites within the RVLM region was also confirmed by autoradiography. These observations are in line with the results of recent studies by other groups which used viral vectors with the same PRSx8 promoter.[31,40] AlstR-EGFP transduced neurones were identified in the RVLM regions occupied by C1 population, thus allowing their reversible inhibition by allatostatin application. Indeed, we demonstrated recently that expression of AlstR mediates immediate silencing of the transduced brainstem neurones following allatostatin applications

regardless of the prevailing CO_2 tension.[28] However, the PRSx8 promoter is also active in the other notable neighbouring neuronal population of chemosensitive Phox2b-expressing RTN neurones, believed to play an important role in the mechanisms underlying CNS respiratory chemosensitivity to changes in PCO_2/pH.[28,41] Indeed, a scatter of EGFP-expressing neurones showing no immunoreactivity for TH was found rostral to the caudal border of the facial nucleus where RTN neurones reside.

Since some of the RTN neurones were transduced with AlstR-EGFP and, therefore, inhibited in the presence of allatostatin,[28] the role of this neuronal population in the generation of sympathetic activity has to be discussed. RTN neurones are glutamatergic[41] and project to the RVLM.[42,43] Consistent with previous reports,[44,45] our data showed that blockade of RTN (and other) inputs to the RVLM presympathetic circuitry following administration of the broad spectrum glutamate receptor antagonist kynurenic acid had no effect on resting sympathetic activity. These data suggest that the C1 neuronal population does not require excitatory glutamatergic inputs from the RTN to generate a significant level of sympathetic vasomotor tone. Our experiments demonstrated that in conditions of ionotropic glutamatergic receptor blockade, inhibition of the RVLM AlstR-EGFP-expressing neurones by allatostatin application still resulted in significant decreases in RSNA and MABP during hypercapnia. In addition, RTN neurones have not been previously implicated in generating sympathetic activity and the observations of Moreira et al.[44] imply that even though a substantial proportion of RTN neurones may have been transduced by PRSx8-AlstR-EGFP-LV, allatostatin-induced effect on sympathetic activity is unlikely to be related to inhibition of these neurones.

Interestingly, systemic hypercapnia in the absence of the peripheral chemoreceptor inputs evoked vigorous increases in SNA, however, the slopes of the CO_2-evoked sympathoexcitatory and cardiovascular responses were not affected following inhibition of C1 neurones (and transduced RTN neurones for that matter). Although, there is evidence that hypercapnia increases discharges of C1 neurones in vivo,[21] recent evidence indicates that these neurones are not pH-chemosensitive when isolated in vitro.[22,23] Together these recent reports and the data obtained in the present study suggest that while providing tonic sympathetic drive, RVLM C1 neurones do not appear to be responsible for increases in SNA evoked by central actions of CO_2. By extension, the major component of the CO_2-evoked sympathetic response must be provided by bulbospinal non-catecholaminergic RVLM neurones or sympathoexcitatory neurones located in other parts of the brain (e.g. rostral ventromedial and midline medulla, the A5 cell group of the pons or the paraventricular hypothalamic nucleus) and/or spinal pre- or even post-ganglionic neurones.

In summary, our data confirm a fundamental physiological function of a distinct population of catecholaminergic C1 neurones of the RVLM. In contrast to previous observations based on the results of the experiments involving chronic and permanent lesions, acute inhibition of AlstR-EGFP-expressing C1 neurones following application of allatostatin reveals that this neuronal group contributes in a significant manner to the maintenance of the sympathetic tone and arterial blood pressure at rest. Although, C1 neurones do not appear to mediate sympathoexcitation evoked by central actions of CO_2, this study provides important guidance for further studies of brain mechanisms underlying increases in sympathetic vasomotor tone, vascular remodelling, and cardiovascular pathology

which accompany disruptions in gas exchange in patients with obstructive sleep apnoea.

References

1. Young T, Peppard PE, Gottlieb DJ. Epidemiology of obstructive sleep apnea: a population health perspective. *Am J Respir Crit Care Med* 2002;**165**:1217–1239.
2. Narkiewicz K, Somers VK. Sympathetic nerve activity in obstructive sleep apnoea. *Acta Physiol Scand* 2003;**177**:385–390.
3. Yamauchi M, Nakano H, Maekawa J, Okamoto Y, Ohnishi Y, Suzuki T et al. Oxidative stress in obstructive sleep apnea. *Chest* 2005;**127**:1674–1679.
4. Young T, Peppard P, Palta M, Hla KM, Finn L, Morgan B et al. Population-based study of sleep-disordered breathing as a risk factor for hypertension. *Arch Intern Med* 1997;**157**:1746–1752.
5. Peppard PE, Young T, Palta M, Skatrud J. Prospective study of the association between sleep-disordered breathing and hypertension. *N Engl J Med* 2000;**342**:1378–1384.
6. Milleron O, Pilliere R, Foucher A, de RF, Aegerter P, Jondeau G et al. Benefits of obstructive sleep apnoea treatment in coronary artery disease: a long-term follow-up study. *Eur Heart J* 2004;**25**:728–734.
7. Yaggi HK, Concato J, Kernan WN, Lichtman JH, Brass LM, Mohsenin V. Obstructive sleep apnea as a risk factor for stroke and death. *N Engl J Med* 2005;**353**:2034–2041.
8. Arzt M, Young T, Finn L, Skatrud JB, Bradley TD. Association of sleep-disordered breathing and the occurrence of stroke. *Am J Respir Crit Care Med* 2005;**172**:1447–1451.
9. Dampney RA, Horiuchi J, Tagawa T, Fontes MA, Potts PD, Polson JW. Medullary and supramedullary mechanisms regulating sympathetic vasomotor tone. *Acta Physiol Scand* 2003;**177**:209–218.
10. Guyenet PG. Neural structures that mediate sympathoexcitation during hypoxia. *Respir Physiol* 2000;**121**:147–162.
11. Guyenet PG, Koshiya N, Huangfu D, Baraban SC, Stornetta RL, Li YW. Role of medulla oblongata in generation of sympathetic and vagal outflows. *Prog Brain Res* 1996;**107**:127–144.
12. Dampney RA. Functional organization of central pathways regulating the cardiovascular system. *Physiol Rev* 1994;**74**:323–364.
13. Madden CJ, Sved AF. Cardiovascular regulation after destruction of the C1 cell group of the rostral ventrolateral medulla in rats. *Am J Physiol Heart Circ Physiol* 2003;**285**:H2734–H2748.
14. Spyer KM. Central nervous mechanisms contributing to cardiovascular control. *J Physiol* 1994;**474**:1–19.
15. Strack AM, Sawyer WB, Hughes JH, Platt KB, Loewy AD. A general pattern of CNS innervation of the sympathetic outflow demonstrated by transneuronal pseudorabies viral infections. *Brain Res* 1989;**491**:156–162.
16. Horiuchi J, Dampney RA. Dependence of sympathetic vasomotor tone on bilateral inputs from the rostral ventrolateral medulla in the rabbit: role of baroreceptor reflexes. *Neurosci Lett* 1998;**248**:113–116.
17. Ross CA, Ruggiero DA, Park DH, Joh TH, Sved AF, Fernandez-Pardal J et al. Tonic vasomotor control by the rostral ventrolateral medulla: effect of electrical or chemical stimulation of the area containing C1 adrenaline neurons on arterial pressure, heart rate, and plasma catecholamines and vasopressin. *J Neurosci* 1984;**4**:474–494.
18. Sun MK. Central neural organization and control of sympathetic nervous system in mammals. *Prog Neurobiol* 1995;**47**:157–233.
19. Sun MK. Pharmacology of reticulospinal vasomotor neurons in cardiovascular regulation. *Pharmacol Rev* 1996;**48**:465–494.
20. Habler HJ, Janig W, Michaelis M. Respiratory modulation in the activity of sympathetic neurons. *Prog Neurobiol* 1994;**43**:567–606.
21. Seller H, Konig S, Czachurski J. Chemosensitivity of sympathoexcitatory neurones in the rostroventrolateral medulla of the cat. *Pflugers Arch* 1990;**416**:735–741.
22. Lazarenko RM, Milner TA, DePuy SD, Stornetta RL, West GH, Kievits JA et al. Acid sensitivity and ultrastructure of the retrotrapezoid nucleus in Phox2b-EGFP transgenic mice. *J Comp Neurol* 2009;**517**:69–86.
23. Gourine AV, Kasymov V, Marina N, Tang F, Figueiredo MF, Lane S et al. Astrocytes control breathing through pH-dependent release of ATP. *Science* 2010;**329**:571–575.

24. Schreihofer AM, Guyenet PG. Sympathetic reflexes after depletion of bulbospinal catecholaminergic neurons with anti-DbetaH-saporin. *Am J Physiol Regul Integr Comp Physiol* 2000;**279**:R729–R742.

25. Birgul N, Weise C, Kreienkamp HJ, Richter D. Reverse physiology in *Drosophila*: identification of a novel allatostatin-like neuropeptide and its cognate receptor structurally related to the mammalian somatostatin/galanin/opioid receptor family. *EMBO J* 1999;**18**:5892–5900.

26. Callaway EM. A molecular and genetic arsenal for systems neuroscience. *Trends Neurosci* 2005;**28**:196–201.

27. Lechner HA, Lein ES, Callaway EM. A genetic method for selective and quickly reversible silencing of Mammalian neurons. *J Neurosci* 2002;**22**:5287–5290.

28. Marina N, Abdala AP, Trapp S, Li A, Nattie EE, Hewinson J et al. Essential role of Phox2b-expressing ventrolateral brainstem neurons in the chemosensory control of inspiration and expiration. *J Neurosci* 2010;**30**:12466–12473.

29. Teschemacher AG, Wang S, Raizada MK, Paton JF, Kasparov S. Area-specific differences in transmitter release in central catecholaminergic neurons of spontaneously hypertensive rats. *Hypertension* 2008;**52**:351–358.

30. Lonergan T, Teschemacher AG, Hwang DY, Kim KS, Pickering AE, Kasparov S. Targeting brain stem centers of cardiovascular control using adenoviral vectors: impact of promoters on transgene expression. *Physiol Genomics* 2005;**20**:165–172.

31. Abbott SB, Stornetta RL, Socolovsky CS, West GH, Guyenet PG. Photostimulation of channelrhodopsin-2 expressing ventrolateral medullary neurons increases sympathetic nerve activity and blood pressure in rats. *J Physiol* 2009;**587**:5613–5631.

32. Coleman JE, Huentelman MJ, Kasparov S, Metcalfe BL, Paton JFR, Katovich MJ et al. Efficient large-scale production and concentration of HIV-1-based lentiviral vectors for use *In vivo*. *Physiol Genomics* 2003;**12**:221–228.

33. Tan W, Janczewski WA, Yang P, Shao XM, Callaway EM, Feldman JL. Silencing preBotzinger complex somatostatin-expressing neurons induces persistent apnea in awake rat. *Nat Neurosci* 2008;**11**:538–540.

34. Gourine AV, Llaudet E, Dale N, Spyer KM. Release of ATP in the ventral medulla during hypoxia in rats: role in hypoxic ventilatory response. *J Neurosci* 2005;**25**:1211–1218.

35. Paton JF. A working heart-brainstem preparation of the mouse. *J Neurosci Methods* 1996;**65**:63–68.

36. Abdala AP, Rybak IA, Smith JC, Paton JF. Abdominal expiratory activity in the rat brainstem-spinal cord *in situ*: patterns, origins and implications for respiratory rhythm generation. *J Physiol* 2009;**587**:3539–3559.

37. Trapp S, Aller MI, Wisden W, Gourine AV. A role for TASK-1 (KCNK3) channels in the chemosensory control of breathing. *J Neurosci* 2008;**28**:8844–8850.

38. Yu CG, Hayes TK, Strey A, Bendena WG, Tobe SS. Identification and partial characterization of receptors for allatostatins in brain and corpora allata of the cockroach *Diploptera punctata* using a binding assay and photoaffinity labeling. *Regul Pept* 1995;**57**:347–358.

39. Chen D, Bassi JK, Walther T, Thomas WG, Allen AM. Expression of angiotensin type 1A receptors in C1 neurons restores the sympathoexcitation to angiotensin in the rostral ventrolateral medulla of angiotensin type 1A knockout mice. *Hypertension* 2010;**56**:143–150.

40. Kanbar R, Stornetta RL, Cash DR, Lewis SJ, Guyenet PG. Photostimulation of Phox2b medullary neurons activates cardiorespiratory function in conscious rats. *Am J Respir Crit Care Med* 2010;**182**:1184–1194.

41. Mulkey DK, Stornetta RL, Weston MC, Simmons JR, Parker A, Bayliss DA et al. Respiratory control by ventral surface chemoreceptor neurons in rats. *Nat Neurosci* 2004;**7**:1360–1369.

42. Rosin DL, Chang DA, Guyenet PG. Afferent and efferent connections of the rat retrotrapezoid nucleus. *J Comp Neurol* 2006;**499**:64–89.

43. Abbott SB, Stornetta RL, Fortuna MG, DePuy SD, West GH, Harris TE et al. Photostimulation of retrotrapezoid nucleus Phox2b-expressing neurons *in vivo* produces long-lasting activation of breathing in rats. *J Neurosci* 2009;**29**:5806–5819.

44. Moreira TS, Takakura AC, Colombari E, Guyenet PG. Central chemoreceptors and sympathetic vasomotor outflow. *J Physiol* 2006;**577**:369–386.

45. Sved AF, Ito S, Yajima Y. Role of excitatory amino acid inputs to the rostral ventrolateral medulla in cardiovascular regulation. *Clin Exp Pharmacol Physiol* 2002;**29**:503–506.